Monolithically Integrated Quantum Cascade Lasers, Detectors and Dielectric Waveguides at 9.5μm for Far-Infrared Lab-on-Chip Chemical Sensing

Yi Zou,[1] Karun Vijayraghavan,[1] Parker Wray,[1] Swapnajit Chakravarty,[2] Mikhail A. Belkin,[1] and Ray T. Chen[1,2]

[1]Microelectronics Research Center, Electrical and Computer Engineering Department, University of Texas at Austin, Austin, TX, 78758, USA
[2]Omega Optics Inc., Austin, TX, 78759, USA
Author e-mail address: swapnajit.chakravarty@omegaoptics.com, mbelkin@ece.utexas.edu, raychen@uts.cc.utexas.edu,

Abstract: We provide the first experimental demonstration of room temperature far-infrared lab-on-chip chemical sensing via monolithic integration of quantum cascade laser, quantum cascade detector and dielectric waveguides at the long infrared wavelength of 9.5μm.
OCIS codes: (300.6270) Spectroscopy, far infrared; (300. 6340) Spectroscopy, infrared; (230.7370) Waveguides;

Infrared (IR) absorption spectroscopy is widely accepted as the ideal technique for chemical sensing due to its capability to distinguish analytes of interest based on unique molecular vibration signatures [1, 2]. Many IR spectroscopy systems require separately integrated optical sources, detectors and gas cells for interactions between light and the analyte. These components together with other free-space optics require careful alignment and assembly, and limits system size to that of table-top or handheld systems. Over the last decade, quantum cascade laser (QCL) sources enabled the transition from off-chip thermal sources to on-chip light sources in the mid- and far-IR wavelengths. Concurrently, long wavelength detectors have achieved commercialization success. In particular the development of quantum cascade detectors (QCD) has culminated in the demonstration of monolithic QCL-QCD chip sized systems that operate at 6.5μm [3].

Lab-on-chip IR absorption spectroscopy demonstrated in the near-IR for the detection of volatile organic compounds [4, 5] and greenhouse gases [6] is governed by the Beer-Lambert-Bouguer law, where the transmitted intensity I is given by

$$I = I_0 \times \exp(-\gamma\alpha L) \quad (1)$$

where I_0 is the incident intensity, α is the absorption coefficient of the medium, L is the interaction length, and γ is the medium-specific absorption factor determined by dispersion-enhanced light–matter interaction. For various free-space based sensors, L must be large to achieve high sensitivity since γ=1. From perturbation theory

$$\gamma \propto f \times \frac{c/n}{n_g} \quad (2)$$

where c is the speed of light in free space, v_g is the group velocity in the medium, n is the refractive index of the medium [7], and f is the filling factor denoting the relative fraction of the optical field residing in the analyte medium. Given that the group velocity v_g is inversely proportional to the group index n_g, the optical absorbance by a waveguide on a same chip increases in order as follows: (a) strip waveguides, (n_g~3) in silicon for instance, (b) slotted strip waveguides (n_g~3, f ~10) since the intensity of light in a low-index slot is significantly enhanced compared to strip waveguides, (c) PCWs (n_g ~100), and (d) slotted PCWs (f ~10 and n_g ~100 for a combined factor of ~1000). In the mid-IR, fundamental vibration signatures of compounds are stronger by two to three orders of magnitude compared to their corresponding overtones in the near-infrared. The increased in the mid-IR combined with the afore mentioned waveguide enhancements should result in mid-IR spectroscopy systems having significantly larger detection sensitivity than near-IR counterparts. We have previously demonstrated detection of triethylphosphate (TEP) at 3.43 μm, and measured 10 ppm (parts per million) with an 800 μm long slotted PCW, compared to only 28 pph (parts per hundred) in a slot waveguide on a silicon-on-sapphire (SoS) platform [8] using external interband cascade lasers (ICL) and detectors interfaced with the SoS chip via mid-IR optical fibers.

It can be expected that at 9.5μm, based on 2 orders of magnitude higher absorbance of TEP, 100ppb detection is feasible. However, several challenges need to be overcome to demonstrate monolithic PCW QCL-QCD platform. Since QCL/QCDs are intersubband devices, the TM-polarized laser emission must be rotated orthogonally to a TE-polarization imposed by the PCW guiding characteristics, and then re-converted back to a TM-polarization for QCD detections. Furthermore, to avoid re-absorption of light from the source laser in the intermediary waveguide, the waveguide must be grown or deposited separate after QCL and QCD fabrication. Authors in ref. [9] consequently integrated a plasmonic waveguide to avoid polarization conversion requirements and achieve sensing at a metal-air

interface. In this paper, as a step towards the ultimate goal of integrating slotted PCWs, we present the first experimental demonstration of the integration of high index germanium waveguides with QCLs and QCDs on InP substrates at 9.5μm. Preliminary chemical sensing data is presented.

Semiconductor multi-quantum-well heterostructures that operate simultaneously as QCL at negative bias and photovoltaic QCD at zero bias were designed, grown, processed, and tested. The structure in Fig. 1 was optimized for high detector performance. The conduction band diagram and electron wavefunctions at a bias voltage of -40 kV/cm (QCL condition) is shown in Fig. 1(a) with electron transport and laser emission indicated schematically. Fig. 1(b) shows the same structure at zero bias voltage (QCD operation) and the principle of operation as a detector is shown schematically. The device consists 35 repetitions of the active region stages shown in Fig. 1 sandwiched between two 3.5μm-thick waveguide layers of low-doped InP. The structure was grown on InP [001] wafer n-doped to ~1-2×10^{18} cm^{-3}.

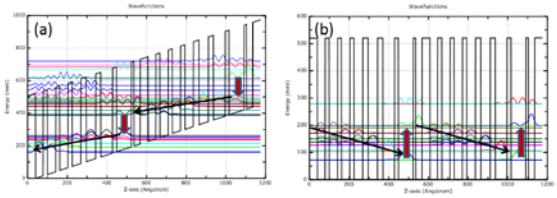

*Fig. 1. Conduction band diagram of two consecutive stages of the active region designed for operation as both QCL and QCD. Structure is grown using AlInAs/InGaAs heterostructure lattice-matched to InP. The layer sequence (in Angstroms), starting from the injection barrier, is **40**/31/**13**/75/**20**/59/**26**/47/**28**/44/**21**/42/**20**/42/**21**/39 where AlInAs barriers are shown in bold and the underlined layers are n-doped to 2×10^{17} cm^{-3}. Panel (a) shows laser operation at applied bias field of -40 kV/cm. Panel (b) shows detector operation of the same structure at zero bias field. Light emission and absorption is shown by thick red downward- and upward-going arrows (respectively), while the electron transport is shown by black arrows.*

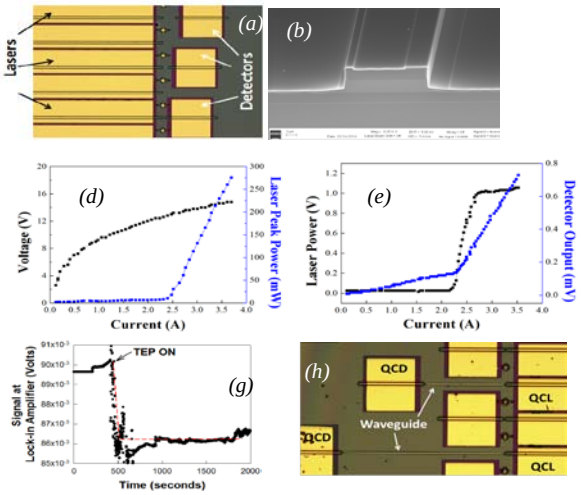

Fig. 2. (a) Microscope image of devices showing fabricated quantum cascade lasers and detectors with different separations, monolithically integrated. (b) SEM image of cleaved facet of quantum cascade laser via which the QCL performance is characterized. (c) Broaband QCL emission spectrum at centered at 9.55μm. (d) Light-current (blue) and current-voltage (black) characteristics of the QCL in (c). (e)Detector output voltage (blue) plotted together with laser power. QCD power seen to increase prior to QCL reaching threshold, due to crosstalk between QCL and QCD via common ground (n-doped substrate). (f)QCD signal plotted as a function of laser bias in air (blue), isopropyl alcohol (IPA) in black and methanol (red). (g) Change in QCD signal in 20μm air gap in presence of 28pph triethylphosphate at 9.5μm. (h) Microscope images of Ge waveguides between QCL and QCD to support TM mode propagation.

Standard fabrication sequence for QCL and QCD was employed and devices are shown in Figs. 2(a) and 2(b). L-I and I-V curves were measured for the QCL with 50 KHz 50ns drive pulses. The detector signal is measured as a function of increasing laser drive voltage for the QCL and QCD separated by 20μm. For larger gaps, QCD detected signal was reduced due to fast divergence of the emitted laser beam. The change in the QCD signal as a function of laser drive voltage was measured for 2 chemicals, IPA and methanol. It was observed that methanol with higher absorbance (0.35) at 9.5μm caused a larger drop in detector signal than IPA (0.08) and air, evidenced by increased slope. While the system of Fig. 2(a) was able to detect TEP in gas phase at 28pph as shown in Fig. 2(g), by the near instantaneous drop in measured power by the QCD in presence of TEP, it was unable to detect in ppm concentrations. As described by Eq. 1 and Eq. 2, 3μm high strip waveguides of different lengths in germanium (Ge) were next fabricated between QCL and QCD. Fig. 2(h) shows a microscope image of a 500μm long and 1mm long Ge waveguides. Measurements are in progress.

In summary, we experimentally demonstrated the monolithic integration of QCL, QCD and dielectric Ge waveguide on InP substrate for operation at 9.5μm. Volatile organic compounds IPA and methanol were detected together with the chemical warfare simulant, triethylphosphate. Further measurements are in progress.

The research was sponsored by US Army ECBC SBIR contract #W911SR-12-C-0046. The authors also thank NSF SBIR (IIP-1127251) for partial support.

References

[1] M. Lackner et al., Rev. Chem. Engg. **23**, 65-147 (2007)
[2] F. Adler, et al., Opt. Express **18**, 21861-21872 (2010)
[3] B. Schwarz, et al., Sensors **13**, 2196-2205 (2013)
[4] W.-C. Lai, et al., Opt. Lett **38**, 3799-3802 (2013)
[5] W.-C. Lai, et al., Appl. Phys. Lett. **98**, 023304 (2011)
[6] W.-C. Lai, et al., Opt Lett **36**, 984-986 (2011)
[7] N. A. Mortensen et al., Appl. Phys. Lett. **90**, 141108 (2007).
[8] Y. Zou et al., concurrent CLEO 2015 submission
[9] B. Schwarz, et al., Nat. Comm. **5:4085**, 1-7 (2014)